Detector-On-Demand for Flexible Homodyne Transmission

Bernhard Schrenk[(1)], and Fotini Karinou[(2)]
[(1)]*AIT Austrian Institute of Technology, Center for Digital Safety&Security / Security & Communication Technologies, 1210 Vienna, Austria.*
[(2)]*Microsoft Research Ltd., 198 Cambridge Science Park, CB4 0GW Cambridgeshire, United Kingdom.*
Author e-mail address: bernhard.schrenk@ait.ac.at

Abstract: We demonstrate a segmented coherent detector configuration that enables polarization-insensitive or -multiplexed reception in half- or full-duplex operation mode for single-λ or ultra-dense WDM configurations with up to 91 Gb/s/sub-λ OFDM data rate.

1. Introduction

With 6G applications looming on the horizon, the metro segment is expected to support Tb/s capacities through a flexible and reconfigurable network [1]. As a prime notion in such optical networks, an adaptation to the highly dynamic bandwidth demand or channel loss, both in terms of a reconfigurable spectral allocation [2-4] or expansion towards the space and polarization dimensions [5], is deeply rooted in the layouts of modern optical transmission systems. Ideally, this goal is accomplished by optical transponders without physically altering or over-provisioning its optical-layer configuration during the lifecycle, calling in return for a very flexible optical transceiver engine.

Towards this direction, we have proven an electro-absorption modulated laser (EML) as full-duplex coherent homodyne transceiver [6]. Here, we expand on these findings by introducing a segmented EAM configuration for low-cost, high-capacity coherent OFDM transmission in various scenarios: We experimentally demonstrate a segmented electro-absorption modulator (EAM) detector architecture and show that a flexible assignment of polarization and spectrum and half-/full-duplex operation modes can be supported. Furthermore, access to the sub-DWDM dimension through balanced detection enables a dense channel allocation with 91.6 Gb/s/sub-λ data rates.

2. Coherent Detector-on-Demand and Experimental Setup

The proposed transceiver features a synthesized detector / modulator engine, with the ability to (*i*) partition RF spectrum towards single-λ full-duplex transmission, (*ii*) double the capacity through access to the polarization dimension and (*iii*) accomplish coherent WDM reception to enhance the spectral efficiency.

Table 1. Detector-on-demand configurations for six scenarios.

Configuration	TRX	BW [GHz]	λ	TX pol.
❶ Half-duplex	DET-1	15 DS	λ_T	TE
❷ Full-duplex bidi	DET-1	6 DS, 6 US	λ_T	TE
❸ Pol. independent	DET-1	15 DS	λ_T	TE scramb.
❹ Pol. multiplexed	DET-2	15 DS	λ_T	TE + TM
❺ Balanced det.	DET-3	15 DS	λ_T	TE
❻ UDWDM	DET-3	15 DS	λ_T, $\lambda_{a1/2}$	TE

Figure 1a presents the experimental setup to evaluate the proposed transceiver (TRX) that will be evaluated in various scenarios (Table 1). It builds on an injection-locked LO with a free-running wavelength of ~1550.46 nm and having a locking range of 5.3 GHz for an injection level of -10 dBm, rendering it stable even for low ROP levels and sub-optimal state of input polarization. The multi-purpose detector/modulator EAM has a -3dB bandwidth of 13.6 GHz and is biased at -1.5V. Three segmented configurations are evaluated: a single-ended inline-EAM (DET-1 in Fig. 1b) that either detects [6] or modulates the TE, TM polarizations at its two inputs, a serialized EAM representation (DET-2 in Fig. 1c) that provides dedicated electrical ports for the TE and TM polarizations, and a balanced EAM (DET-3 in Fig. 1d). All these configurations could be realized simultaneously through four EAM sections, so that a definition of the TRX function then occurs at the electrical domain and without change at the optical layer. For example, bidirectional full-duplex operation of DET-1 can be facilitated through slicing the RF spectrum for the EAM through a RF duplexer (DPX). It shall be noted that

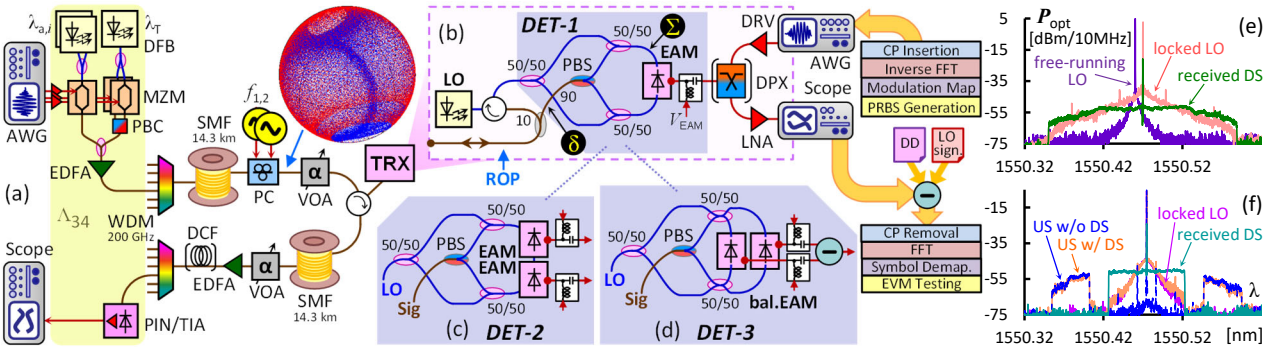

Fig. 1. (a) Experimental setup and detector architectures for (b) single-ended EAM and (c) segmented EAM and (d) balanced EAM detectors. The inset shows the polarization-scrambled DS signal. Optical spectra for (e) half-duplex 15-GHz DS and (f) full-duplex 6-GHz DS/US transmission.

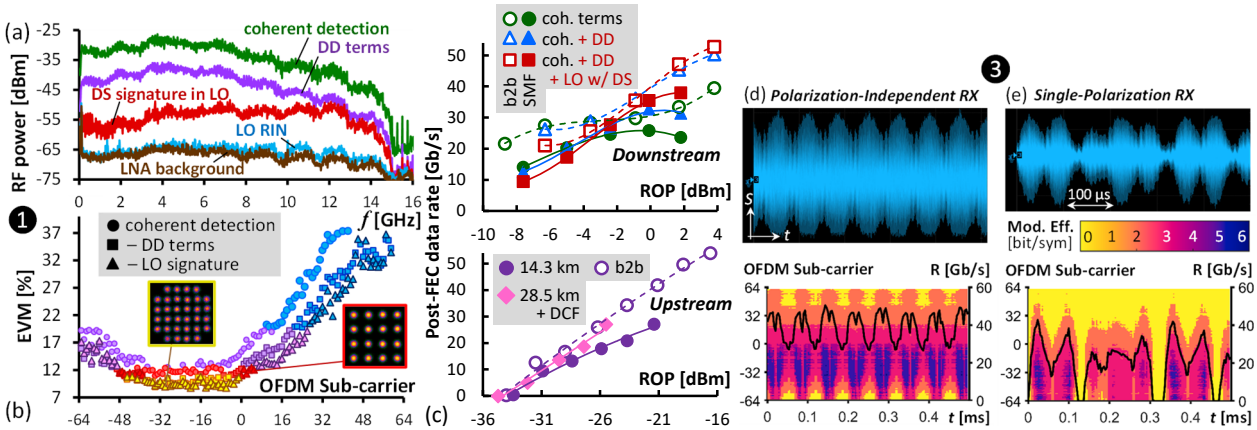

Fig. 2. (a) 15-GHz DS spectra and (b) b2b EVM. (c) OFDM rate vs ROP. (d) Polarization-independent and (e) single-polarization DS reception.

injection-locked LO provides optical frequency and phase synchronization to the received signal. However, the use of fiber-pigtailed components leads to inevitable phase fluctuations. To mitigate these, we availed of environmental stabilization, a 2-kHz linewidth laser at the head-end (λ_T) and fiber stretchers between the signal and LO paths within the TRX, controlled by feedback on the detected RF spectrum. The 128 sub-carriers of the single-polarization and polarization-multiplexed OFDM downstream (DS) are adaptively bit loaded. Two closely-spaced adjacent channels ($\lambda_{a,1/2}$) are provisioned at the ITU-channel 34 for the balanced detection case, together with the DS channel λ_T at 1550.47 nm, to which the LO of the TRX unit is optically locked. Polarisation scrambling is applied to investigate polarization-indepedent TRX operation. A pre-amplified PIN/TIA receiver detects the upstream (US). Figure 1e shows the optical spectra for half-duplex 15-GHz DS reception and the filtering effect when injection-locking the LO. Figure 1f shows the shared spectrum among a full-duplex 6-GHz DS and 6-GHz US.

3. Results and Discussion

Figures 2a/b report the RF spectra and EVM for single-λ, single-polarization *half-duplex* back-to-back (b2b) 15-GHz DS reception with *single-ended EAM* detector (DET-1 in Fig. 1b) at a ROP of 1.8 dBm. At this high ROP level, direct-detection (DD) terms are significant and lead to an EVM degradation, resulting in an average modulation efficiency of 2.41 bit/sym (●) for optimized bit loading. When applying a time-synchronized feed-forward cancellation of separately recorded DD terms, the modulation efficiency would improve to 3.28 bit/sym (■). At the same time, residual DS components contaminate the locked LO, especially in a region beyond the injection-locking range. We cancelled this LO signature by feeding forward a respective recording taken after interrupting the DS signal at point δ in Fig. 1b. The modulation efficiency then improves to 3.41 bit/sym (▲), which equates to an OFDM data rate of 47.1 Gb/s. Besides direct OFDM demodulation and additional feed-forward cancellation, which has been applied for the sake of investigating penalties, no further DSP methods were required to accomplish homodyne OFDM reception, as proven through the clean sub-carrier constellations in Fig. 2b.

Figure 2c presents the DS performance as a function of the ROP. For b2b transmission, we can identify the single-ended TRX architecture as a limiting factor towards higher ROP (○) due to the relatively wide gap to the reception case insensitive to DD-terms (△). For transmission over 14.3 km, the penalty in data rate (■,□) is attributed to chromatic dispersion. Figure 2c further discusses the half-duplex 15-GHz US transmission performance when using the EAM exclusively as transmitter. We obtain an OFDM data rate of 53 Gb/s for a ROP of -17 dBm at the EDFA+PIN based US receiver (○). Dispersion-induced fading quickly deteriorates the performance, leading to a ~40% penalty in peak rate for 14.3 km SMF transmission (●). This penalty is due to chromatic dispersion, as proven through a DCF-assisted (-425 ps/nm) US receiver when transmitting over 28.5 km with negligible rate penalty (◆).

The *polarization-independent* TRX operation is proven in Fig. 2d for driving the polarization controller (PC) simultaneously at $f_{1,2}$ = 15 and 6 kHz. This results in a scrambled polarization state for the received DS (Fig. 1a) during its block-wise OFDM demodulation. While for the polarization-diversity TRX architecture the data rate varies in a range between 26.5 and 50.4 Gb/s, we see an expected drop in modulation efficiency down to 0 bit/sym in case of a single-polarization TRX (Fig. 2e), for which one EAM port has been left disconnected (Σ in Fig. 1b).

Figure 3a presents the RF spectra at the EAM-based DS and EDFA+PIN based US receivers for *full-duplex* b2b DS/US transmission for a DS ROP of -0.5 dBm, together with the transfer function T_{DPX} of the RF duplexer at the TRX. Without US, the received 6-GHz DS features a good EVM performance with a modulation efficiency of 5.23 bit/sym (Fig. 3b, ●). This corresponds to a data rate of 29 Gb/s. When activating the US, a crosstalk note can be noticed towards the edge of the DS band of the DPX (Fig. 3a). Still, the crosstalk is bearable even though the US is ~5 orders-of-magnitude stronger. In this case of simultaneous US transmission at the upper RF band, the modulation

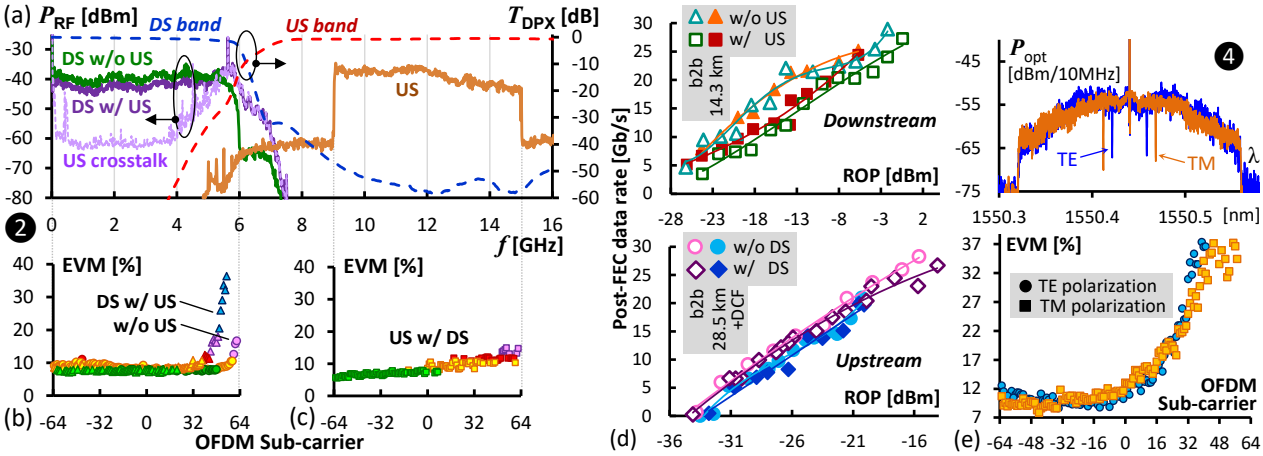

Fig. 3. (a) Full-duplex DS/US RF spectra and EVM for (b) DS and (c) US. (d) OFDM rate vs ROP. (e) Polarization-multiplexed DS reception.

efficiency of the DS drops slightly to 4.93 bit/sym (Fig. 3b, ▲). An OFDM rate of 27.3 Gb/s is supported. This proves the successful wavelength-sharing of DS and US. The modulation efficiency obtained for US transmission was 4.82 bit/sym (■) for a ROP of -17 dBm at the EDFA+PIN US receiver, equivalent to a rate of 26.7 Gb/s (Fig. 3c).

Figure 3d summarizes the OFDM rates for DS (▲,■) and US (●,◆) for b2b and fiber transmission. When compared to the half-duplex 6-GHz DS, we see a rate penalty of 9-35% for full-duplex transmission (▲,■) over the entire range of ROP. Due to the reduced signal bandwidth of 6 GHz, there is no additional dispersion-induced penalty. The US performance is widely independent of the presence of DS data. Concerning chromatic dispersion, similar conditions apply as for the half-duplex 15-GHz US transmission (Fig. 2c) since the US is spectrally allocated to the upper RF band.

Figure 3e shows *polarisation-multiplexed* reception with the segmented EAM of DET-2 (Fig. 1c). We transmitted two 15-GHz DS signals with a distinctive notch at one OFDM sub-carrier in the TE, TM polarizations and aligned the input polarization to the TRX for optimal separation. The EVM, taken for a ROP of 4 dBm, shows average modulation efficiencies of 3.41 and 3.21 for TE and TM, permitting 91.6 Gb/s reception in total.

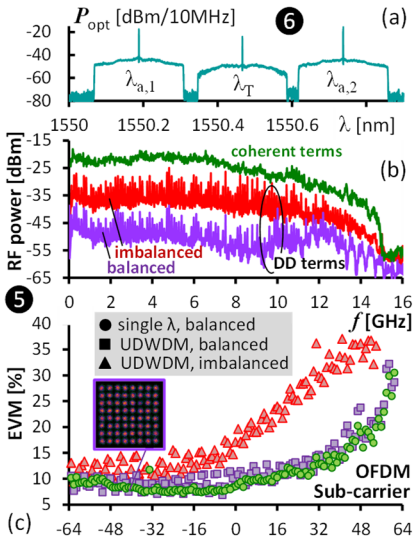

Fig. 4. (a) Optical spectra, (b) DD terms and (c) EVM for balanced EAM detector configuration.

Figure 5 proves the *balanced EAM* operation (DET-3 in Fig. 1a) for DS reception in an ultra-dense, 34-GHz spaced WDM scheme within channel Λ_{34} (Fig. 4a). We see an improvement of ~14 dB in average for the suppression of DD terms and adjacent channel noise (Fig. 4b). The penalty arising from the adjacent channels $\lambda_{a,1/2}$ (▲ in Fig. 4c) in terms of modulation efficiency can be entirely recovered through the balanced EAM configuration (■), permitting a single-polarization data rate of 58.8 Gb/s for a ROP of 4 dBm, similar to the rate of 62.4 Gb/s obtained for single-channel transmission at λ_T (●) within Λ_{34}. The balanced EAM detector does not require digital compensation concerning DD terms or the DS signature in the LO.

4. Conclusion

We have experimentally evaluated EAM technology to synthesize a multi-purpose modulator/detector for a variety of coherent reception and transmission functions with increased flexibility in the use of optical (λ, polarization) and electrical (RF spectrum) network resources. We have demonstrated polarization-multiplexed, full-duplex and UDWDM modes through such a segmented EAM configuration in combination with a synchronized LO for coherent OFDM reception. Future work will comprise of the photonic integration of the segmented detector.

Acknowledgement: This work was supported by the ERC under the EU Horizon-2020 programme (grant agreement No 804769).

5. References

[1] L.S. de Sousa et al., "Metropolitan optical networks: A survey on single-layer architectures" Opt. Switching and Netw. **47**, 100719 (2023).
[2] W. Shieh, "OFDM for Flexible High-Speed Optical Networks," JLT **29**, 1560 (2011).
[3] L. Nadal et al., "SDN-Enabled Multi-Band S-BVT Within Disaggregated Optical Networks," JLT **40**, 3479 (2022).
[4] D. Welch et al., "Digital Subcarrier Multiplexing: Enabling Software-Configurable Optical Networks," JLT **41**, 1175 (2023).
[5] C. Wang et al., "Optical Slicing to Enhance Application Performance over a Metro Transport Network," Proc. OFC, W4F.5 (2022).
[6] B. Schrenk, "The Electroabsorption-Modulated Laser as Optical Transmitter and Receiver: Status and Opportunities", Optoel. **14**, 374 (2020).